

Direct generation and amplification of ultra-broadband noise-like pulse in an all-PM Tm-doped fiber laser system

Desheng Zhao, Xiran Zhu, Zhanxuan Wu, Jiawei Wang, Xiang Li, Long Tian, Lirong Chen, Yaohui Zheng

Abstract—An ultra-broadband noise-like pulse (NLP) directly emitted from an all polarization-maintaining (all-PM) fiber laser is reported, for the first time. The fiber laser is designed as a figure-of-eight cavity and relies on nonlinear amplifying loop mirror for mode-locking. A phase shifter is used to ensure the self-starting capability of the fiber laser. By enhancing the intracavity positive feedback and nonlinear response, a linearly polarized ultra-broadband NLP is obtained with spectral coverage of 1900.2 nm to 2367.3 nm, corresponding to a 30 dB spectral width of 418.2 nm. The average power and pulse energy of the achieved NLP are 90.4 mW and 16.86 nJ, respectively. Then, an all-PM single-stage cladding-pumped amplifier is utilized to boost the power to 14.4 W and broaden the spectrum to >2400 nm, the corresponding pulse energy is 2.68 μ J. Such μ J-levels, all-PM, cost-effective and easy-to-integrate fiber laser system is an excellent pump source for linearly polarized optical coherence tomography and supercontinuum generation.

Index Terms—Mode-locking fiber laser, Tm-doped, noise-like pulse, ultra-broadband.

I. INTRODUCTION

2 μ m pulsed fiber lasers have important application prospects in many high-precision measurements, industrial processing and medical surgery, due to the characteristics of the 2 μ m wavelength band and the advantages of fiber laser [1-4]. For example, some water absorption peaks are located in 2 μ m band, allowing 2 μ m pulsed fiber lasers to be widely used in medical surgery [5]. Taking advantage of the 2 μ m laser's high atmospheric transmissivity, long-distance space communication is available [6, 7]. In particular, 2 μ m broad-spectrum pulse plays a very important role in optical

coherence tomography (OCT), supercontinuum generation and wide-spectrum imaging applications. OCT technology based on 2 μ m broadband pulse light source can enhance the probing depth of low water content and highly scattering materials [8]. Mid-infrared supercontinuum seeded by 2 μ m broadband spectrum pulse has significant advantages in broadening the spectral width and improving the conversion efficiency [9]. Above applications have attracted the interest of many researchers in the generation of 2 μ m broadband spectrum pulse [10].

Direct output of noise-like pulse (NLP) from fiber laser is an effective scheme to obtain broadband spectral laser. The NLP with dual-scale configuration bundles a large number of femtosecond to picosecond soliton pulses in a single envelope, and has a broad and smooth spectrum feature. However, the low nonlinearity and gain of the fiber and the high insertion loss of the fiber components prevent the easy realization of broadband NLP at 2 μ m and longer wavelengths. To obtain broadband NLP, Sobon et al. used a normal dispersion fiber with a small core in Tm-doped fiber laser, the 10 dB bandwidth of the obtained NLP reaches 300 nm [11]. Li et al. employed a microfiber to obtain an NLP with a 10 dB spectral width of 151 nm in a nonlinear polarization evolution (NPE) Tm-doped fiber laser [12]. To date, almost all reports focus on obtaining broadband NLP in non-polarization-maintaining (non-PM) fiber laser, which usually require the manipulation of intracavity polarization state. The non-PM configuration reduces the environmental interference resistance of fiber laser. From the practical application perspective, a 2 μ m all-PM fiber laser is necessary because of its higher stability and ability to output linearly polarized laser. However, the realization of a broadband NLP all-PM fiber laser at 2 μ m is difficult. In the all-PM configuration, mode-locking is achieved based on material saturable absorber, nonlinear polarization evolution (NPR) as well as nonlinear amplifying loop mirror (NALM) [13]. However, material saturable absorbers have the disadvantages of low damage threshold and poor long-term stability. NPR/NPE mode-locking implementation in all-PM structure mainly relies on splicing of polarization-maintaining fibers at different angles [14, 15]. This necessitates substantial empirical substantiation, and the varied angular splicing exacerbates the intracavity loss, hindering the realization of mode-locking at 2 μ m. In contrast, the NALM technique has become the conventional solution for all-PM fiber laser as it

Manuscript received xx xx, 2024; revised xx xx, 2024; accepted xx xx, 2024. Date of publication xx xx, 2024; date of current version xx xx, 2024. This work was supported in part by the National Natural Science Foundation of China (NSFC), China (Grant Nos. No. 62225504, No. U22A6003, No. 62035015). (Corresponding authors: Long Tian; Yaohui Zheng.)

Desheng Zhao, Zhanxuan Wu, Jiawei Wang, Xiang Li, Long Tian, Lirong Chen and Yaohui Zheng are with the State Key Laboratory of Quantum Optics Technologies and Devices, Institute of Opto-Electronics, Shanxi University, Taiyuan 030006, China and the Collaborative Innovation Center of Extreme Optics, Shanxi University, Taiyuan 030006, China. (e-mail: deshengzhao@sxu.edu.cn; 202422609011@email.sxu.edu.cn; 202412607019@email.sxu.edu.cn; 202222607026@email.sxu.edu.cn; tianlong@sxu.edu.cn; clr@sxu.edu.cn; yhzhang@sxu.edu.cn).

Xiran Zhu is with the Beijing Institute of tracking and telecommunications technology, Beijing 100094, China. (e-mail: zxiran@126.com)

relies only on the intensity interference within the coupler to achieve mode-locking. Despite the NALM cavity configuration's inherent disadvantage of poor self-starting capability, this limitation can be mitigated by a phase shifter that introduces a linear phase shift supplementing NALM mode-locking. This method has been used extensively in ultrafast laser generation [16, 17]. Therefore, NALM mode-locking combined with a phase shifter guarantees the realization of NLP in all-PM fiber laser. To obtain the broadband NLP in all-PM fiber laser, the low nonlinearity as well as the difficulty and costly fabrication of polarization-maintaining highly nonlinear fibers and components at 2 μm is the other challenge. Hence, it is necessary to investigate new access solution for low-cost and easy integration of linearly polarized broadband NLP laser. Further, in order to satisfy high power demands, NLP can realize power enhancement through amplifier.

In this paper, we have not only achieved the first linearly polarized ultra-broadband NLP for the first time but also successfully boost its average power to 14.4 W by employing an all-PM amplifier. Self-starting mode-locking operation is achieved using a commercially available polarization-maintaining phase shifter (PM-PS). The realization of ultra-broadband NLP is mainly dependent on the combined effect of intracavity-enhanced positive feedback and nonlinear response. The linearly polarized ultra-broadband NLP has a spectral range covering from 1900.2 nm to 2367.3 nm. The 30 dB spectral bandwidth is 418.2 nm and the output power is 90.4 mW. Relying on an all-PM cladding pumped amplification structure, the power of the NLP is boosted to 14.4 W, which corresponds to a pulse energy of 2.68 μJ . The spectrum of the ultra-broadband NLP is further broadened to over 2400 nm during the amplification process. The power fluctuation in the tested one-hour period is 0.26%, demonstrating that the fiber laser system has a good stability.

II. EXPERIMENT STRUCTURE

The structure of the ultra-broadband NLP all-PM fiber laser and single-stage amplifier is displayed in Fig. 1. As depicted in Fig. 1(a), the fiber laser is organized in a figure-eight configuration with NALM ring and unidirectional ring (UR). A polarization-maintaining optical coupler (PM-OC 1) connects the two rings to form NALM mode-locking. The pump source in the NALM ring consists of a 1550 nm seed laser and a single-stage amplifier. The 1550 nm fiber laser system is capable of outputting 4.3 W continuous wave laser and pumps a 3.2 m polarization-maintaining Tm-doped fiber (PM-TDF, given in Table 1) via a 1550 nm/2000 nm fused polarization-maintaining wavelength division multiplexer (PM-WDM). For self-starting mode-locking operation, a PM-PS with a $\text{Pi}/2$ linear phase shift is placed after the PM-TDF. A section of passive fiber (PM1550/PM1950 fiber) in the UR is utilized to increase the intracavity nonlinearity and guarantee the broadband NLP output. A polarization-maintaining isolator (PM-ISO 1) and a PM-OC 2 are used for the unidirectional transmission of the laser in the cavity and the output, respectively. To reduce the loss induced

by the broadband NLP spectrum passing through the PM-ISO, the passive fiber is placed between the PM-ISO and PM-OC 2.

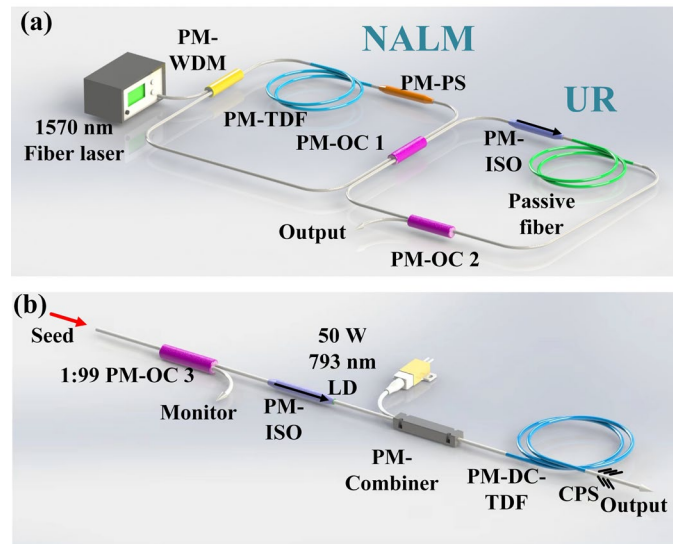


Figure 1. Schematic of (a) all-PM ultra-broadband NLP fiber laser and (b) single-stage all-PM amplifier.

To further broaden the spectrum and boost the power of broadband NLP, an all-PM single-stage amplifier is connected after the fiber laser. A PM-OC 3 is utilized to monitor the output state of the fiber laser. A PM-ISO 2 with a power handling of 10 W is inserted between the PM-OC 3 and the amplifier to protect the fiber laser. The single-stage amplifier employs a forward cladding pumping scheme in which a 50 W multimode 793 nm laser diode (LD) pumps a 3 m length polarization-maintaining double-clad Tm-doped fiber (PM-DC-TDF, given in Table 1) via a polarization-maintaining combiner. A section of matched passive fiber is fused after the PM-DC-TDF and a home-made cladding pump stripper (CPS) dumps the residual pump laser. The end of the passive fiber is cut at an angle of 8° to reduce the effect of the backward light on the amplifier and fiber laser. The output characteristics of the fiber laser and amplifier are evaluated by an optical spectrum analyzer (OSA) with a measurement range of 1200 nm-2400 nm, a real-time oscilloscope with a bandwidth of 4 GHz, an autocorrelator with a sweep range of 50 ps, a power meter with a power handling of 60 W and a radio frequency (RF) spectrum analyzer with a detection range of 2 Hz-8 GHz.

Table 1. Parameters of polarization-maintaining gain fibers

	PM-TDF	PM-DC-TDF
Core/Cladding Diameters	9/125 μm	10/130 μm
Core NA	0.15	0.14
Cladding NA	/	≥ 0.46
Birefringence	2.5×10^{-4}	2.5×10^{-4}
Cladding Absorption	/	3.2 dB/m at 793 nm
Core Absorption	9.0 dB/m at 1180 nm	/

III. RESULTS AND DISCUSSION

A. Initial pulse characteristics of the fiber laser

In the initial configuration of the fiber laser, 55 m PM1550 fiber is utilized, along with 30:70 PM-OC 1 and 20:80 PM-OC 2 with 20% port as the output. Due to the incorporation of intra-cavity polarization-maintaining fibers and components, the polarization state within the cavity becomes fixed, rendering adjustment through a polarization controller impractical. Consequently, mode-locking in this setup is achieved solely through the tuning of the pump power. Experimentally increasing the pump power to 2 W, a stable pulse train can be achieved. It is worth noting that fiber laser only outputs continuous wave in the absence of PM-PS. The evolutions of the output spectra and pulse waveforms are exhibited in Fig. 2. The spectral width of the mode-locking pulse gradually broadens with the continuous increase of the pump power, the corresponding 30 dB spectral width increases to 148.9 nm. The center wavelength of the mode-locking pulse at the maximum pump power is 1977.4 nm. In the time domain, the pulse waveform broadens to 3.04 ns without a significant increase in amplitude intensity.

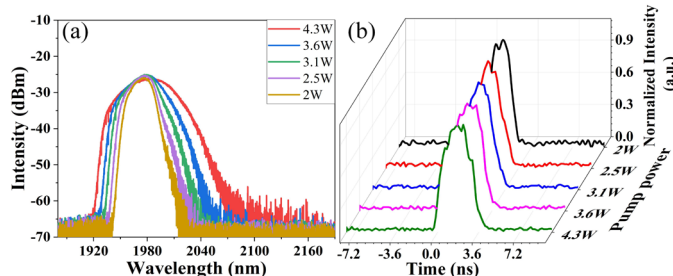


Figure 2. The characteristics of the mode-locking pulse. (a) Spectral curve. (b) Time-domain waveform.

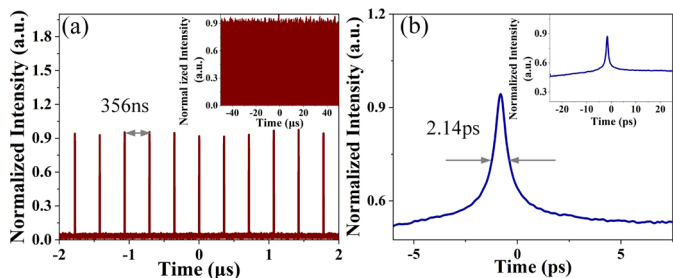


Figure 3. At maximum pump power, (a) pulse trains in different time ranges; (b) AC traces in the 15 ps range and 50 ps range.

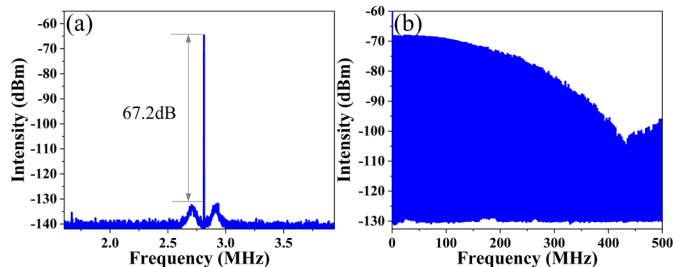


Figure 4. RF spectra in (a) 2.3 MHz and (b) 500 MHz at pump power of 4.3 W.

The pulse sequences and AC traces at maximum pump power of 4.3 W are displayed in Figs. 3(a) and 3(b), respectively. The adjacency interval of the pulses is 356 ns, which corresponds to the time that the pulse propagates once in the cavity. The absence of disorganized pulses between

adjacent pulse demonstrates that the obtained pulse is operating in a single-pulse state. A larger range of pulse sequence is exhibited in the inset of Fig. 3(a), where the mode-locking pulse train has a low intensity fluctuation. An interference spike is present in the AC trace when the sub-pulses are existing inside the pulse envelope, as depicted in Fig. 3(b). The AC trace of the pulse has a width of 2.14 ps, indicating that a large number of soliton pulses with an average full width at half height of 2.14 ps in the envelope. This confirms that the built laser is operating in the NLP regime [18, 19]. As displayed in Fig. 4, the measured repetition frequency is 2.812 MHz consistent with the pulse propagation time within the cavity and the signal-to-noise ratio (SNR) of the NLP is 67.2 dB. The wide range of RF spectrum indicates good stabilization of the NLP.

B. Optimization of NLP spectral width

To enable the direct output of ultra-broadband NLP from the fiber laser, we experimentally optimize the multidimensional parameters of the cavity that enhance the intracavity positive feedback and nonlinear response. The coupling ratio of intracavity PM-OC 2 is firstly optimized, as illustrated in Fig. 5(a). By increasing the coupling ratio of the PM-OC 2 (i.e., lower output proportion), the peak power of the pulses injected into the NALM ring is improved and the higher peak power is able to excite more spectral broadening due to the enhanced nonlinear response [20]. As a result, we obtain an NLP with a 30 dB spectral width of 287.1 nm at 10:90 PM-OC 2.

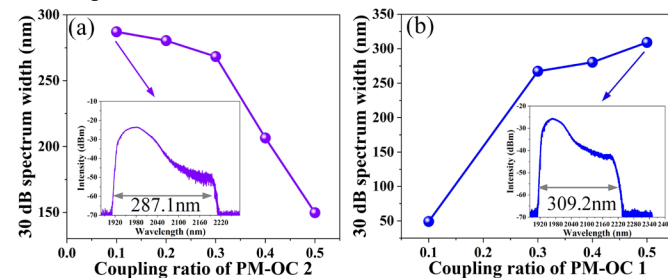


Figure 5. The 30 dB spectrum widths of different coupling ratios of (a) PM-OC 2 and (b) PM-OC 1. Inset: NLP spectra.

We then investigate the effect of the coupling ratio of the PM-OC 1 connecting the two rings on the output spectrum. Increasing the coupling ratio of PM-OC 1 improves the peak power for NLP formation. In this case, the intracavity positive feedback is enhanced and the critical saturation power value of the NALM is raised. The peak power of the soliton amplified by the TDF can experience a more rapidly growth, together with a narrower pulse width, and the corresponding spectral width broadens further. Then, pulse collapse occurs, resulting in the formation of an NLP with a broader spectrum. Thus, the 30 dB spectral width of the NLP increases to 309.2 nm with an increase in the coupling ratio to 0.5 (i.e., 50:50). The corresponding spectral range of the NLP is able to cover from 1899.6 nm to 2240.7 nm, as displayed in the inset of Fig. 5(b). With the replacement of PM-OC 1 with a larger coupling ratio, the fiber laser is only able to output a continuous wave due to the fact that the mode-locking threshold power is higher than the pump power.

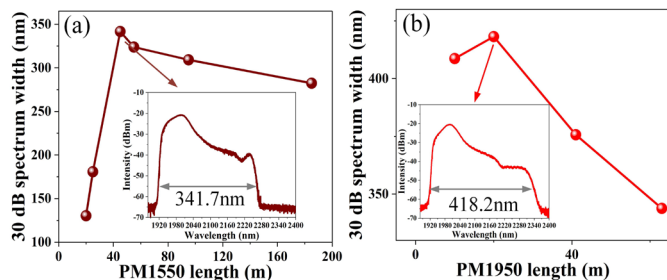


Figure 6. The 30 dB spectral widths at different passive fiber lengths, (a) PM1550 and (b) PM1950 fibers. Inset: Spectra at the maximum 30 dB spectral width.

The intracavity passive fiber has an important influence on the spectral width, which includes two parameters of fiber type and length. We optimize the lengths and types of the intracavity passive fiber under the coupling ratios of PM-OC 1 and PM-OC 2 of 50:50 and 10:90, respectively. As displayed in Fig. 6(a), increasing the length of the PM1550 fiber enhances the nonlinear response in the cavity, which excites more nonlinear effect induced spectral broadening and enables spectral extension to longer wavelengths. As a result, the 30 dB spectral width of the NLP increases from 130.4 nm to 341.7 nm when the length of the PM1550 fiber is increased from 20 m to 45 m. The NLP spectrum can cover from 1918.2 nm to 2259.9 nm at the maximum 30 dB spectral width. However, when further increasing the length of the PM1550 fiber, the percentage of the long-wavelength component of the NLP spectrum decreases and the corresponding 30 dB spectral width reduces to 282.4 nm. This is caused by the larger propagation loss associated with longer PM1550 fiber. Compared to PM1550 fiber (8.5/125 μm), PM1950 fiber (7/125 μm) has a larger nonlinear coefficient, favoring more spectral broadening induced by nonlinear effects at short fiber length. On the other hand, the transmission loss of laser in PM1950 fiber is lower than that in PM1550 fiber, especially for the long-wavelength component of NLP transmitted in fiber [21]. Figure 6(b) exhibits the evolution of the 30 dB spectral width of the NLP with PM1950 fiber length. Similar to the evolution of the spectral width with PM1550 fiber length, the broadest NLP is obtained at a PM1950 fiber length of 20 m and the NLP spectrum is able to cover from 1900.2 nm to 2367.3 nm. Compared to the use of the optimized PM1550 fiber, the 30 dB spectral width increases from 341.7 nm to 418.2 nm.

C. Pulse features of optimized ultra-broadband NLP

By optimizing the intra-cavity multi-dimensional parameters, an ultra-broadband NLP with a 30 dB spectral width of 418.2 nm is experimentally obtained under an PM-OC 1 coupling ratio of 50:50, an PM-OC 2 coupling ratio of 10:90, a PM1950 fiber length of 20 m. The pulse characteristics of the optimized NLP are exhibited in Fig. 7. Figure 7(a) exhibits the spectral evolution versus pump power. As the pump power rises, the proportion of long-wave components in the NLP spectrum gradually increases, the 30 dB spectral width increases from 302.7 nm to 418.2 nm, and there is no continuous wave and other components appearing on the spectrum. The trend of NLP average power versus pump power is plotted in Fig. 7(b). The average power increases linearly to 90.1 mW and the slope

efficiency of the fiber laser is 2.2%. The waveforms and RF spectra at maximum pump power are displayed in Figs. 7(c) and 7(d), respectively. The pulse width is 626 ps. The pulse interval is 187 ns which is inversely proportional to the repetition frequency of the pulse. The RF spectrum of the ultra-broadband NLP shows a SNR of 62.2 dB and a repetition frequency of 5.36 MHz. The large-range RF spectrum is illustrated in the inset of Fig. 7(d), demonstrating that the NLP has good stability.

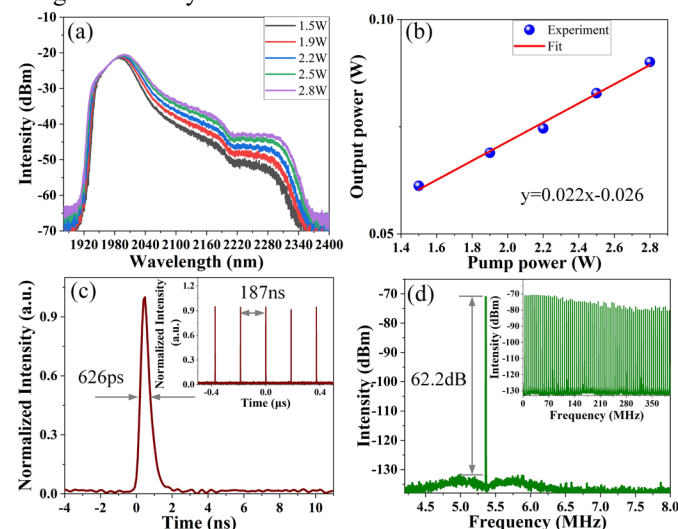


Figure 7. The variations of (a) spectra and (b) power with pump power. (c) Pulse train and (d) RF spectra in different measuring range.

To further characterize the stability of the fiber laser, the power fluctuation over an hour is tested, as depicted in Fig. 8. The average power is 90.9 mW and the power fluctuation is 0.11%, confirming the good power stability of the fiber laser.

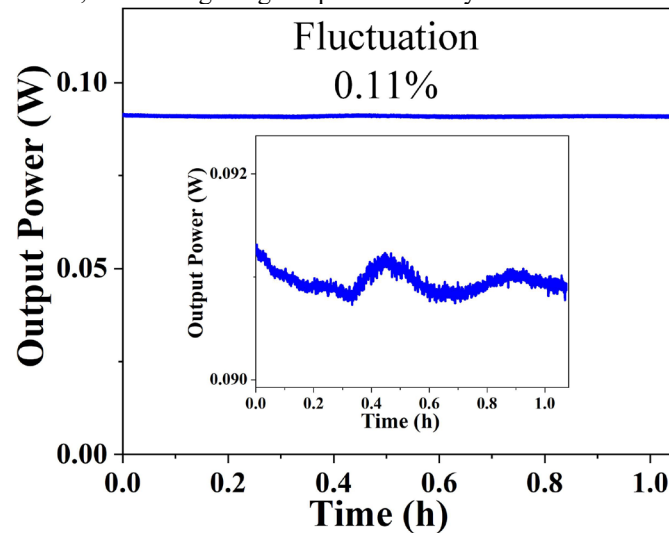


Figure 8. Power stability in 1 hour. Inset: Enlarged detail.

D. The amplified characterization of ultra-broadband NLP

Restricted by the power handling of the fiber components in the fiber laser, it is difficult to achieve high power and spectrum expansion of the NLP. In this case, an external amplifier is needed to improve the performance of the NLP laser. In the experiment, an NLP with an average power of 14.4 W is realized by a single-stage all-PM fiber amplifier. The evolution of the output power is plotted in Fig. 9(a). The average power

linearly scales as the injected 793 nm pump power increases, with a slope efficiency of 29.8%. The spectra at different output powers are presented in Fig. 9(b). Due to the employment of PM-ISO 3 between the fiber laser and the amplifier as well as the high propagation loss of long-wavelength laser in the fiber, the spectral coverage is only from 1933.2 nm to 2211.0 nm at output power of 1.1 W. By further increasing the output power to 14.4 W, the spectrum is able to broaden to over 2400 nm. The practical spectral coverage of the amplified NLP is difficult to observe due to the limitation of the measuring range of the OSA. A wide range of pulse train is depicted in Fig. 9(c), the absence of strong pulse fluctuation indicates that the amplified NLP still has high stability.

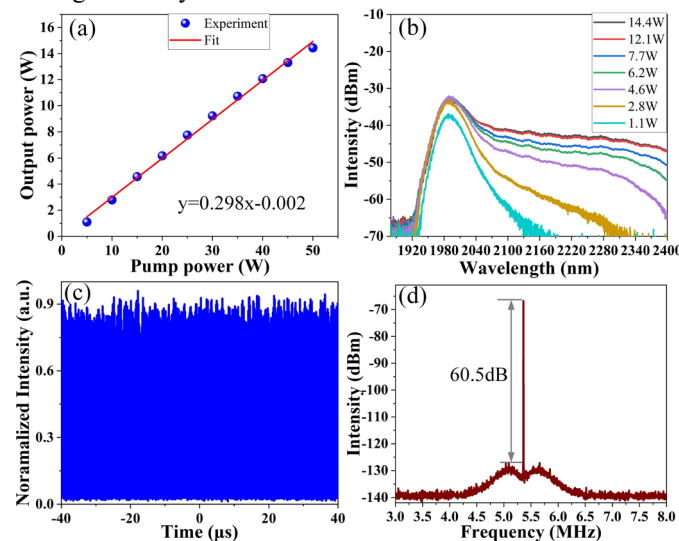


Figure 9. The variations of (a) output power and (b) amplified spectra with 793 nm pump power. (c) Pulse train in 80 μ s range. (d) RF spectrum at the maximum 793 nm pump power.

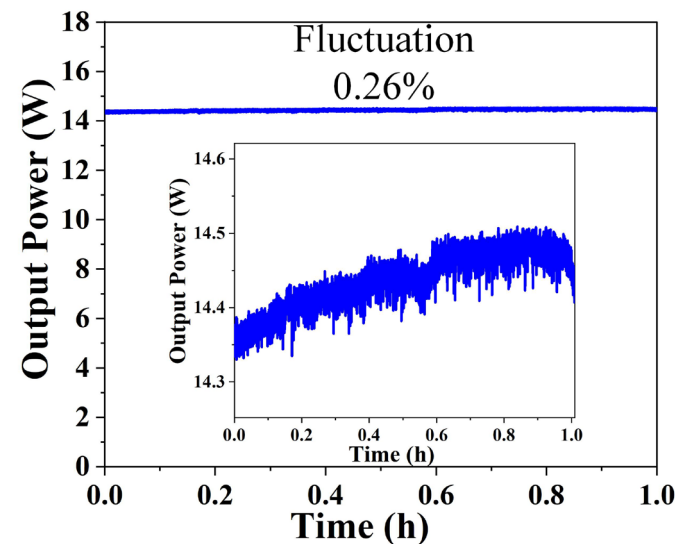


Figure 10. Power stability of the amplifier in 1 hour. Inset: Enlarged detail.

The measured SNR is obtained as illustrated in Fig. 9(d), showing a slight degradation of 60.5 dB due to the introduction of noise in the amplification process. The stability of the amplifier at 14.4 W output power is further monitored as displayed in Fig. 10. The power fluctuation is 0.26%, demonstrating the good power stability of the amplifier.

E. Discussion

In order to achieve ultra-broadband NLP generation, it is necessary to use fibers with high nonlinearity or special components within the Tm-doped fiber laser, which are significantly different from NLP generation at other wavelengths. The utilization of highly nonlinear polarization maintaining fibers or specialized components is constrained by the challenges of their difficult fabrication processes and high costs. Especially at long wavelengths, the spectral broadening induced by nonlinear effects requires higher nonlinearity. This is because the nonlinearity coefficient is wavelength dependent and is calculated as [22]:

$$\gamma = \frac{2\pi n_2}{\lambda A_{eff}}$$

where, n_2 is the fiber nonlinear-index coefficient. λ is the operating wavelength, and A_{eff} is the effective mode area. Longer wavelength leads to lower nonlinearity, further increasing the difficulty of fabricating fibers with high nonlinearity and special components at 2 μ m. Combined with high intracavity loss and low gain at 2 μ m, making it more challenging to generate ultra-broadband NLP in 2 μ m all-PM fiber laser.

To overcome such limitation, we propose a simple, novel structural scheme. First, in 2 μ m all-PM fiber laser, the NALM technique is selected to achieve mode-locking and a PM-PS placed in the NALM ring is utilized to ensure the self-starting of the NLP. Although mode-locking can be established by using passive fiber in the NALM ring, the broadening of the NLP's spectrum is limited by the transmission loss of the passive fiber when the ultra-broadband NLP propagates cyclically in the NALM ring. In our experiments, we use a 20 m PM1550 fiber to replace the PM-PS, the spectral width of the output NLP is much narrower than that of the NLP obtained based on the PM-PS. Moreover, the longer the passive fiber used in the NALM ring, the narrower the spectrum output from PM-OC 2. Therefore, the utilization of a PM-PS is necessary in realizing linearly polarized ultra-broadband NLP.

Second, we enhance the effect of intracavity positive feedback on NLP formation. In an anomalous dispersion cavity, NLP formation is associated with soliton collapse and positive feedback [23]. Under the effect of positive feedback, the peak power of the soliton increases rapidly. Influenced by intracavity gain, nonlinearity, and dispersion, the soliton pulse collapses before its peak power reaches critical saturation power [24]. In this case, intracavity solitons are continuously destroyed and generated. Under the strong pumping force, such a process occurs repeatedly and reaches a balance to form the NLP. This means that the fiber laser working regime evolves from the fundamental soliton mode-locking regime to the NLP regime through the parameter design of the fiber laser. In contrast to non-PM NLP fiber laser, the polarization state of all-PM fiber laser cannot be adjusted by polarization controller. For this reason, we use a segment of PM1550 fiber and a high power 1570 nm pump laser to ensure the formation of NLP. Meanwhile, we enhance the positive feedback effect by changing the coupling ratio of PM-OC 1 to further increase the peak power of the soliton pulses, thereby enabling the NLP to have a wider spectrum. Then, we improve the intracavity

nonlinear response. The broadband NLP generation requires sufficient nonlinear response in the cavity to excite more new spectral components. Therefore, we optimize the coupling ratio of the PM-OC 2 and the length of the passive fiber to enhance intracavity nonlinear response for obtaining a linearly polarized ultra-broadband NLP with a 30 dB spectral width of 418.2 nm. Table 1 summarizes the recent advances of broadband NLP. As can be seen from the Table 1, we report the first scheme for generating ultra-broadband NLP from an all-PM fiber laser.

Table 2. Summary of broadband NLP emitted from fiber laser

Mode-locking	Dopant	Structure	Spectrum width	Reference
NPR	Tm	non-PM	300 nm (10 dB)	[11]
NPR	Er	non-PM	294 nm (3 dB)	[25]
NPE	Tm	non-PM	151 nm (10 dB)	[12]
NPR	Yb	non-PM	290 nm (3 dB)	[26]
NPE	Yb	non-PM	400 nm (30 dB)	[27]
NPR	Tm	non-PM	126 nm (3 dB)	[28]
NALM	Tm	all-PM	418.2 nm (30 dB) >475 nm (30 dB, amplified)	This work

The experimental results also show that lowering the coupling ratio of the output coupler results in a broader spectrum of NLP. However, a smaller proportion of the power is extracted outside the cavity, resulting in a reduction of the output power of the ultra-broadband NLP, as depicted in Fig. 11(a). The output power of NLP decreases from 322 mW to 135 mW as the coupling ratio of PM-OC 2 decreases to 0.1. As the key component of mode-locking, PM-OC 1, the variation of the coupling ratio affects the mode-locking threshold power and output power. Increasing the coupling ratio of PM-OC 1 broadens the spectral range of the NLP. Unfortunately, the corresponding output power is decreased from 174 mW to 113 mW, as plotted in Fig. 11(b). This is because the higher peak power of the NLP mode-locking requires more pump power to be injected into the cavity, which makes the mode-locking threshold rise. Also, NLP with wider spectral output from the fiber laser have lower slope efficiency. To obtain broadband NLP, the use of passive fiber within the UR is especially necessary. Considering the transmission loss of NLP in the passive fiber, optimization of the length of the passive fiber results in the broadest spectrum of NLP. The use of PM1950 fiber with higher nonlinearity and lower transmission loss obviously extends the spectral range of the NLP. However, the fusion splice loss between PM1950 fiber and PM1550 fiber is large. Further expansion of the spectral range of the NLP is

possible by replacing the pigtail of the optical components with PM1950 fiber.

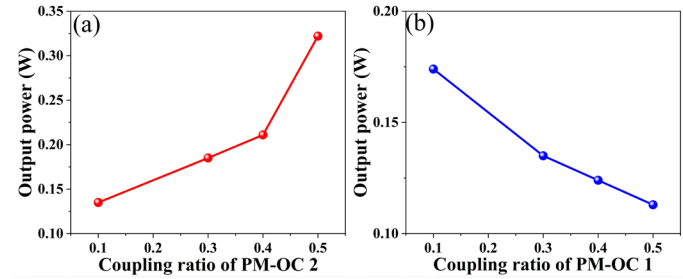


Figure 11. The variations of (a) output power and (b) amplified spectra with 793 nm pump power.

An all-PM amplifier is employed to achieve a power increase together with a spectral broadening to >2400 nm, which also exceeds the current reported spectral range of all-PM NLP amplifier. Due to the high propagation loss of laser with wavelength over 2.4 μm in silica fiber, it is difficult to further increase the spectral coverage of the NLP by constructing an all-PM multi-stage amplifier [29]. Thus, a fluoride fiber-based polarization-maintaining amplification system is necessary to achieve the spectral expansion into the mid-infrared range.

IV. CONCLUSIONS

In conclusion, we have reported an ultra-broadband NLP emitted from an all-PM fiber laser and amplified in an all-PM amplifier. In the all-PM fiber laser, the direct generation of ultra-broadband NLP is achieved by enhancing the intracavity positive feedback and nonlinear response, which is mainly carried out by changing the intracavity passive fiber lengths and the coupling ratio of the PM-OCs. This avoids the complexity and costly nature of polarization-maintaining special fibers and components. The obtained ultra-broadband NLP has a spectral coverage from 1900.2 nm to 2367.3 nm and a 30 dB spectral width of 418.2 nm. The output power of the all-PM fiber laser is 90.4 mW, which corresponds to a pulse energy of 16.86 nJ. The power and pulse energy are boosted by an all-PM single-stage amplifier to 14.4 W and 2.68 μJ , respectively. The spectral coverage of the amplified NLP extends to over 2400 nm, the widest spectral range of all-PM NLP amplifier. The designed system is capable of generating important applications in the fields of optical coherence tomography, industrial processing, and so on.

ACKNOWLEDGMENT

The authors would like to thank Zhichao Luo of South China Normal University for his kind help with this paper.

REFERENCES

- [1] J. Lahyani, M. Thiers, F. Gibert, D. Edouart, J. L. Gouët, and N. Cézard, "Hybrid fiber/bulk laser source designed for CO₂ and wind measurements at 2.05 μm ," *Optics Letters*, vol. 49, no. 4, pp. 969-972, 2024.
- [2] R. E. Tench, C. Romano, J. M. Delavaux, R. Lenox, D. Byrne, and K. Carney, "In-Depth Studies of the Spectral Bandwidth of a 25 W 2 μm Band PM Hybrid Ho- and

- Tm-Doped Fiber Amplifier," *Journal of Lightwave Technology*, vol. 38, no. 8, pp. 2456-2463, 2020.
- [3] L. Gao, L.-a. Zheng, B. Lu, S. Shi, L. Tian, and Y. Zheng, "Generation of squeezed vacuum state in the millihertz frequency band," *Light: Science & Applications*, vol. 13, no. 1, p. 294, 2024/10/17 2024.
- [4] E. Agrell *et al.*, "Roadmap on optical communications," *Journal of Optics*, vol. 26, no. 9, p. 093001, 2024/07/17 2024.
- [5] Y. Lin *et al.*, "Realizing enhanced lithotripsy efficiency using 700 W peak power thulium-doped fiber laser," *Optics & Laser Technology*, vol. 179, p. 111267, 2024/12/01/ 2024.
- [6] Y. Yang, J. Cai, Y. Song, Z. Wang, W. Wu, and J. Ji, "PAM4-modulated 2-micron band for enhanced indoor optical communications: experimental evaluation," *Optics Express*, vol. 32, no. 16, pp. 28012-28024, 2024/07/29 2024.
- [7] Q. Qin *et al.*, "Demonstration of the First Outdoor 2- μm -Band Real-Time Video Transmission Free-Space Optical Communication System Using a Self-Designed Single-Frequency Fiber Laser," *Journal of Lightwave Technology*, vol. 41, no. 16, pp. 5275-5283, 2023.
- [8] C. S. Cheung, J. M. O. Daniel, M. Tokurakawa, W. A. Clarkson, and H. Liang, "High resolution Fourier domain optical coherence tomography in the 2 μm wavelength range using a broadband supercontinuum source," *Optics Express*, vol. 23, no. 3, pp. 1992-2001, 2015/02/09 2015.
- [9] X. Luo *et al.*, "All-Fiber Mid-Infrared Supercontinuum Generation Pumped by Ultra-Low Repetition Rate Noise-Like Pulse Mode-Locked Fiber Laser," *Journal of Lightwave Technology*, vol. 40, no. 14, pp. 4855-4862, 2022/07/15 2022.
- [10] X. Zhu *et al.*, "Spectrally flat mid-infrared supercontinuum pumped by a high power 2 μm noise-like pulse," *Optics Express*, vol. 31, no. 8, pp. 13182-13194, 2023.
- [11] G. Sobon, J. Sotor, T. Martynkien, and K. M. Abramski, "Ultra-broadband dissipative soliton and noise-like pulse generation from a normal dispersion mode-locked Tm-doped all-fiber laser," *Optics Express*, vol. 24, no. 6, pp. 6156-6161, 2016/03/21 2016.
- [12] Y. Li, Y. Kang, X. Guo, and L. Tong, "Simultaneous generation of ultrabroadband noise-like pulses and intracavity third harmonic at 2 μm ," *Optics Letters*, vol. 45, no. 6, pp. 1583-1586, 2020.
- [13] K. Y. Lau, Z. Luo, J. Lin, B. Xu, X. Liu, and J. Qiu, "Development of Figure-of-Nine Laser Cavity for Mode-Locked Fiber Lasers: A Review," *Laser & Photonics Reviews*, vol. n/a, no. n/a, p. 2301239, 2024/09/23 2024.
- [14] X. Liu, F. Ye, M. Zhao, B. A. Malomed, H. Y. Fu, and Q. Li, "All-Polarization-Maintaining Linear Cavity Fiber Lasers Mode-Locked by Nonlinear Polarization Evolution in Stretched Pulse Regime," *Journal of Lightwave Technology*, vol. 41, no. 15, pp. 5107-5115, 2023.
- [15] Y. Jiang *et al.*, "976 nm all-polarization-maintaining mode-locked fiber laser based on nonlinear polarization evolution," *Optics Express*, vol. 31, no. 9, pp. 15170-15178, 2023/04/24 2023.
- [16] B. Ren, C. Li, T. Wang, K. Guo, and P. Zhou, "Stable noise-like pulse generation from a NALM-based all-PM Tm-doped fiber laser," *Optics Express*, vol. 30, no. 15, pp. 26464-26471, 2022/07/18 2022.
- [17] J. Wen *et al.*, "Watt-level all polarization-maintaining femtosecond fiber laser source at 1100 μm ," *Optics Express*, vol. 32, no. 6, pp. 9625-9633, 2024/03/11 2024.
- [18] S. Kobtsev and A. Komarov, "Noise-like pulses: stabilization, production, and application," *JOSA B*, vol. 41, no. 5, pp. 1116-1127, 2024.
- [19] J.-X. Chen *et al.*, "1.7- μm dissipative soliton Tm-doped fiber laser," *Photonics Research*, vol. 9, no. 5, p. 873, 2021.
- [20] A. Komarov, K. Komarov, and L. Zhao, "Mechanism of formation of noiselike pulses in passively mode-locked fiber lasers," *Physical Review A*, vol. 100, no. 3, p. 033829, 09/23/ 2019.
- [21] R. E. Tench *et al.*, "Two-Stage Performance of Polarization-Maintaining Holmium-Doped Fiber Amplifiers," *Journal of Lightwave Technology*, vol. 37, no. 4, pp. 1434-1439, 2019.
- [22] J. Zhao, L. Li, L. Zhao, D. Tang, and D. Shen, "Cavity-birefringence-dependent h-shaped pulse generation in a thulium-holmium-doped fiber laser," *Optics Letters*, vol. 43, no. 2, pp. 247-250, 2018/01/15 2018.
- [23] D. Y. Tang, L. M. Zhao, and B. Zhao, "Soliton collapse and bunched noise-like pulse generation in a passively mode-locked fiber ring laser," *Optics Express*, vol. 13, no. 7, pp. 2289-2294, 2005/04/04 2005.
- [24] Y. Jeong, L. A. Vazquez-Zuniga, S. Lee, and Y. Kwon, "On the formation of noise-like pulses in fiber ring cavity configurations," *Optical Fiber Technology*, vol. 20, no. 6, pp. 575-592, 2014/12/01/ 2014.
- [25] X. Wang *et al.*, "Generation of noise-like pulses with 203 nm 3-dB bandwidth," *Optics Express*, vol. 27, no. 17, pp. 24147-24153, 2019/08/19 2019.
- [26] X. Li, S. Zhang, J. Liu, and Z. Yang, "Using Reverse Saturable Absorption to Boost Broadband Noise-Like Pulses," *Journal of Lightwave Technology*, vol. 38, no. 14, pp. 3769-3774, 2020/07/15 2020.
- [27] J. Zhou, Y. Li, Y. Ma, Q. Yang, and Q. Liu, "Broadband noise-like pulse generation at 1 μm via dispersion and nonlinearity management," *Optics Letters*, vol. 46, no. 7, pp. 1570-1573, 2021.
- [28] J. Liu, X. Li, S. Zhang, D. Yan, and C. Wang, "Broad-spectrum noise-like pulse and Q-switched noise-like pulse in a Tm-doped fiber laser," *Optics & Laser Technology*, vol. 148, p. 107716, 2022.
- [29] S. D. Jackson, "Mid-infrared fiber laser research: Tasks completed and the tasks ahead," *APL Photonics*, vol. 9, no. 7, 2024.